Journal of Applied Polymer Science

Cellulose acetate ultrafiltration membranes reinforced by cellulose nanocrystals: Preparation and characterization

Jianjun Zhou,[1] Jin Chen,[1] Ming He,[1] Jianfeng Yao[2]
[1]College of Science, Nanjing Forestry University, Nanjing 210037, China
[2]College of Chemical Engineering, Nanjing Forestry University, Nanjing 210037, China
Correspondence to. M. He (E-mail: nanjinghm@126.com) and J. Yao (E-mail: jfyao@njfu.edu.cn)

ABSTRACT: Cellulose nanocrystals (CNCs) were used as a sustainable additive to improve the hydrophilicity, permeability, antifouling, and mechanical properties of blend membranes. Different CNC loadings (0–1.2 wt %) in cellulose acetate (CA) membranes were studied. The blend membranes were prepared by a phase-inversion process, and their chemical structure and morphological properties were characterized by attenuated total reflectance–Fourier transform infrared spectroscopy, scanning electron microscopy, porosity, and mean pore size and contact angle measurement. The blend membranes became more porous and more interconnected after the addition of CNCs. The thickness of the top layer decreased and a few large holes in the porous substrate appeared with increasing CNC loading. In comparison with the pure CA membranes, the pure water flux of the blend membranes increased with increasing CNC loading. It reaches a maximum value of 76 $L\,m^{-2}\,h^{-1}$ when the CNC loading was 0.5 wt %. The antifouling properties of the CA membrane were significantly improved after the addition of CNCs, and the flux recovery ratio value increased to 68% with the addition of 0.5 wt % CNCs. In comparison with that of the pure CA membranes, the tensile strength of the composite membranes increased by 47%. This study demonstrated the importance of using sustainable CNCs to achieve great improvements in the physical and chemical performance of CA ultrafiltration membranes and provided an efficient method for preparing high-performance membranes. © 2016 Wiley Periodicals, Inc. J. Appl. Polym. Sci. **2016**, *133*, 43946.

KEYWORDS: biopolymers and renewable polymers; blends; functionalization of polymers; membranes

Received 25 February 2016; accepted 22 May 2016
DOI: 10.1002/app.43946

INTRODUCTION

Membrane separation has attracted considerable attention because of its advantages, including the simple equipment, easy operation, low energy consumption, and lack of pollution. As a green and energy-efficient separation technology, ultrafiltration has been widely used in ultrapure water production, industrial wastewater treatment, and the concentration and purification of biological agents. However, the adsorption and precipitation of biomacromolecule on ultrafiltration membranes causes membrane fouling, which shortens the life of membrane modules and increases costs.[1–3] The prevention of membrane fouling has become a key issue that needs to be solved in the entire membrane process. Modifications of existing membrane materials, such as with plasma treatment, the atomic transfer radical polymerization technique, the synthesis of tailored polymers, and grafting, are frequently performed.[4–6] The membranes used in ultrafiltration are usually made from polymers, such as cellulose acetate (CA), poly(ether sulfone), poly(ether imide), and polysulfone.[7] CA is a commonly used, low-cost ultrafiltration material that is known for its low price, good biocompatibility, and hydrophilicity.[8,9] However, CA membranes are currently used commercially in very limited number because they have low oxidation and chemical resistances, poor mechanical strength, and poor resistance to biological pollution.[10] To improve the hydrophilicity, permeability, and other properties of CA membranes, many studies have been carried out; these studies have included physical blending, chemical grafting, and surface modification.[11–14] Among these methods, physical blending is an easy and efficient method. The blending of CA with an appropriate polymer is expected to produce enhanced separation performance, such as a higher flux and better selectivity.[15]

Cellulose is the most abundant renewable polymer resource in the biosphere; it has many advantages, including biodegradability, low cost, and environmental friendliness. Cellulose nanocrystals (CNCs) exhibit a very high strength and high hydrophilicity when they are prepared by chemical or physical methods.[16] With a diameter of more than 10 nm and a length of tens to hundreds of nanometers, CNCs have a large length-to-diameter ratio, a high strength and stiffness, a large specific surface area, and outstanding electrical and optical properties.

Compared with inorganic nanoparticles, CNCs have received much attention because of their efficiency in improving hydrophilicity and mechanical strength and their low density and reproducibility. Therefore, CNCs in nanoscale are very popular for reinforcing polymers and for enhancing hydrophilicity in the preparation of composite materials.[17,18] Previous studies have reported the reinforcing effect of CNCs on several kinds of polymers, including poly(ethylene oxide), poly(methyl methacrylate), poly(propylene carbonate), poly(L-lactic acid), and polyurethane.[19]

In this study, CNCs were blended with CA to fabricate blend CNC/CA ultrafiltration membranes via a phase-inversion method in a water coagulation bath. Polyvinylpyrrolidone (PVP) was used as a hydrophilic polymeric additive to enhance membrane performance. The effects of the CNC loading (from 0 to 1.2 wt %) on the physical properties and separation performance of the blend membranes were investigated.

EXPERIMENTAL

Materials

Commercial CA and microcrystalline cellulose (MCC) were purchased from Sinopharm Group Chemical Reagent Co. (Shanghai, China) and used without any pretreatment. *N,N*-Dimethylacetamide (DMAc), sulfuric acid (98%), and ethanol were purchased from Nanjing Chemical Reagent Co. (Nanjing, China). Bovine serum albumin (BSA) was purchased from Huixing Biochemical Reagent Co. (Shanghai, China). PVP (25,000 g/mol) was received from Aladdin Industrial Corp. (Shanghai, China).

Preparation of the CNCs

The CNCs were prepared by the acid-catalyzed hydrolysis of MCC. An amount of 20 g of MCC was mixed with 175 mL of sulfuric acid (63.5%) and stirred at 45 °C for 1.5 h. The acid was removed by washing and four to five centrifugation cycles, and then, the residual sulfuric acid was removed by dialysis with deionized water for 72 h until neutrality was reached. The suspensions were freeze-dried for 48 h and then dried in a vacuum oven at 45 °C for 24 h.

Preparation of the Blend Membranes

The pure CA membranes and blend membranes were prepared by a Loeb–Sourirajan phase-inversion process according to the literature[20] with DMAc as the solvent instead of N-methyl-2-pyrrolidone (NMP). Various CA/PVP/DMAc solutions with 15 wt % CA, 2 wt % PVP, and different concentration of CNC (0, 0.2, 0.5, 0.8, and 1.2 wt %) were prepared. The CNC was first introduced into the DMAc solvent. After ultrasonic treatment for 1 h at 600 W, CA and additive PVP polymer were quickly introduced. The casting solution was obtained after the mixture was stirred at ambient temperature for 4 h and then kept still for 12 h. The solution was cast on a glass plate substrate with a stainless scraper. After exposure in air for 30 s, the glass plate was quickly immersed in a gelation bath (deionized water). The membrane sheets were subsequently stored in deionized water for 24 h to remove the residual solvent before the tests.

Membrane Characterization

Transmission electron microscopy (TEM) was performed on a JEM-1400 electron microscope operating at 80 kV. A suspension of nanocellulose was deposited on a Cu grid and left under an IR lamp for 2 min and to evaporate the water. The grid was then stained with a 2% uranyl acetate in water solution for 5 min and dried before analysis.

Fourier transform infrared (FTIR) spectra of the CNC powders prepared by the KBr pellet technique and attenuated total reflectance (ATR)–FTIR spectra of the membrane samples were measured with a VERTEX-70 (Bruker, Germany) spectrometer. The pure CA and CNC/CA blend membranes and CNC powder were completely dried at 50 °C *in vacuo* for 24 h before analysis.

Scanning electron microscopy (SEM) images were observed by Quanta 200 (FEI). The membranes were snapped in nitrogen liquid to obtain a generally clean break for the cross-sectional scan. The mechanical properties, including the tensile strength and elongation at break, of the membranes were determined under ambient conditions on a universal testing machine (SUNS CMT5504, China) at a speed of 20 mm/min. The wet membranes were first freeze-dried and then cut into rectangular shapes (15 × 100 mm^2).[21] The hydrophilicity of the prepared membranes was analyzed to test the contact angle between water and the membranes with contact angle measurements (G10, KRŰSS, Germany). To minimize the experimental error, the contact angle was measured at five random locations for each sample, and the average value was recorded.[22]

Pure Water Flux and Rejection Ratio Testing

The pure water flux of the membrane was tested after the membrane was precompressed with pure water for 30 min at a pressure of 0.1 MPa. The flux was measured under steady-state conditions according to the method described by Chen and Sun.[23] The pure water flux (J_w; $L\,m^{-2}\,h^{-1}$) is defined as the volume of water (V; L) permeated through a membrane of area A (m^2) in a time interval t (h):

$$J_w = V/(At) \tag{1}$$

The rejection ratio of the BSA solution (1 g/L) was tested under a working pressure of 0.1 MPa, and the absorbances of the permeate and feed solutions were measured at 280 nm with a UV-1200 spectrophotometer. The rejection of BSA was calculated by the following equation[24]:

$$\text{Rejection}\ (\%) = \left[1-\left(C_p/C_f\right)\right] \times 100 \tag{2}$$

where C_p and C_f are the protein concentrations of the permeate and feed solutions, respectively.

Water Content, Porosity, and Mean Pore Size Testing

The membrane was cut into a fixed size, weighed in the hygroscopic state, and then dried in an oven to a constant weight.[25] The water content was calculated with the following equation:

$$\text{Water content}\ (\%) = [(W_w - W_d)/W_w] \times 100 \tag{3}$$

where W_w is the weight of the wet membrane (g) and W_d is the weight of the dry membrane (g). The porosity and mean pore size of the membranes were tested according to the method reported by Zhang and coworkers:[25,26]

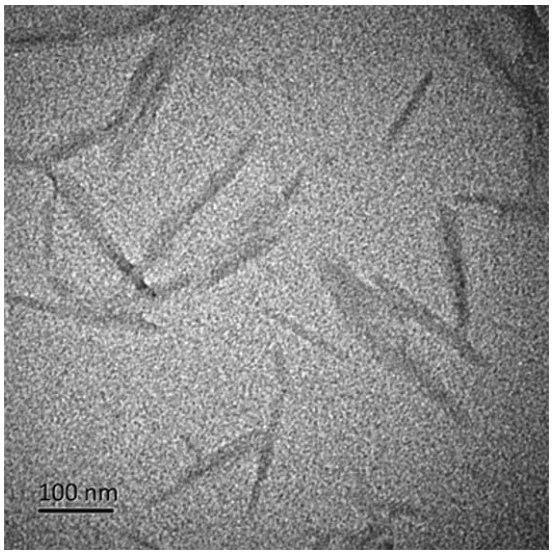

Figure 1. TEM image of CNCs.

$$\text{Porosity } (\%) = [(W_w - W_d)/(d_w \times A_m \times L_m)] \times 100 \quad (4)$$

where d_w is the water density (g/cm^3) and A_m and L_m are the membrane area (cm^2) and thickness (cm), respectively. The mean pore size of the membranes was defined as r_m and calculated with the following equation:

$$r_m = \sqrt{\frac{(2.9 - 1.75P_r) \times 8\eta l J_w}{3600 P_r \times \Delta P}} \quad (5)$$

where P_r is the porosity (%), η is the water viscosity at 25 °C (8.9×10^{-4} Pa s), l is the membrane thickness (m), and ΔP is the operation pressure (Pa).

Fouling Resistance Testing

The prepared pure CA membrane and blend membranes were subjected to fouling resistance studies by means of the measurement of the flux recovery ratio (FRR).[10] The antifouling properties of the membranes was tested with a 1 g/L BSA solution. For this study, the initial pure water flux for an unused membrane was recorded as J_{w1}. The pure water was then replaced by the BSA solution, and its flux was recorded for 30 min (J_p). The BSA-fouled membranes were first flushed and then mechanically washed with deionized water to remove the weakly adhered BSA molecules from the membrane surface, after which the pure water flux for 30 min was recorded again as J_{w2}. The FRR was calculated with the following equation:

$$\text{FRR } (\%) = (J_{w2}/J_{w1}) \times 100 \quad (6)$$

Surface fouling and internal membrane fouling was assessed in terms of the reversible fouling ratio (R_r) and irreversible fouling ratio (R_{ir}):[27]

$$R_r(\%) = \left[\left(J_{w2} - J_p\right)/J_{w1}\right] \times 100 \quad (7)$$

$$R_{ir}(\%) = [(J_{w1} - J_{w2})/J_{w1}] \times 100 \quad (8)$$

RESULTS AND DISCUSSION

Structure and Morphology of the Membrane

The CNCs were observed by TEM (Figure 1), and the crystals had a sticklike structure with lengths of about 100–200 nm and diameters of about 20–30 nm. Figure 2(a) shows the FTIR spectrum of CNCs. The absorptions at 3340, 2900, 1640, and 1430 cm^{-1} were related to the O—H stretching vibrations of cellulose, C—H stretching vibrations of cellulose, bending vibrations of absorbing H—O—H groups, and CH_2 scissor bending vibrations of cellulose, respectively; these were in conformity with the characteristic cellulose absorption peak position.[28] Compared with the pure CA membrane [Figure 2(b)], the ATR–FTIR spectrum of the CNC/CA composite membrane [Figure 2(c)] showed an obvious band at 3340 cm^{-1}, which was attributed to the absorption of the O—H stretching vibrations of cellulose; this suggested that the CNCs existed in the composite membranes.[29]

Figure 3 shows the cross-sectional SEM images of the membranes prepared with different amounts of CNCs. All of the membranes exhibited a typical asymmetric structure with a skin layer on top and a porous substrate. As shown in Figure 3(a,b), the porous substrate showed more interconnection after the addition of 0.2 wt % CNC. In addition, the thickness of the skin layer decreased, and the pore volume in the porous substrate increased with increasing CNC content from 0.2 to 1.2 wt % [Figure 3(b–d)]. This was because the CNC played an important role in accelerating the process of instantaneous phase separation during the immersion process, and this sped up the generation of the polymer-poor phase, and thus, structures with large pores were formed.[30] Figure 3(a1–d1) shows the amplified SEM images of the cross-sectional membranes. The spongylike structure gradually became compact compared with the pure CA membrane. We noticed further that some irregular pores appeared when 1.2 wt % CNC was added. The irregular pores may have been evidence of CNC agglomeration in the diffusion process.

Figure 4 shows the surface SEM images of the membranes prepared from the pure CA and CNC/CA (0.5 wt %). The top surface of the pure CA membrane, where a smooth membrane surface was formed, is shown in Figure 4(a). Figure 4(b) shows that CNC particles were incorporated into polymers to form an uneven surface.14 Figure 4(c,d) shows the bottom-surface SEM

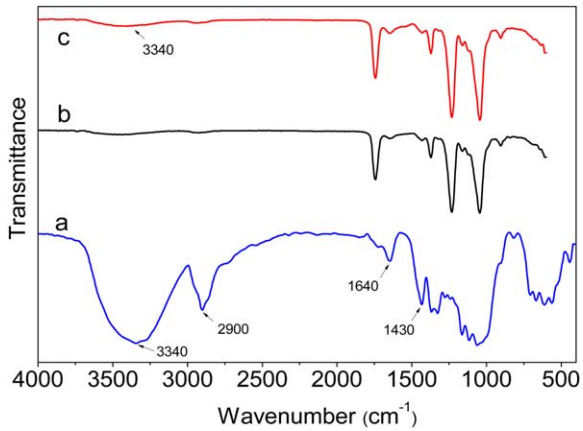

Figure 2. (a) FTIR spectra of the CNCs and ATR–FTIR spectra of the (b) pure CA membranes and (c) CNC/CA blend membranes. [Color figure can be viewed in the online issue, which is available at wileyonlinelibrary.com.]

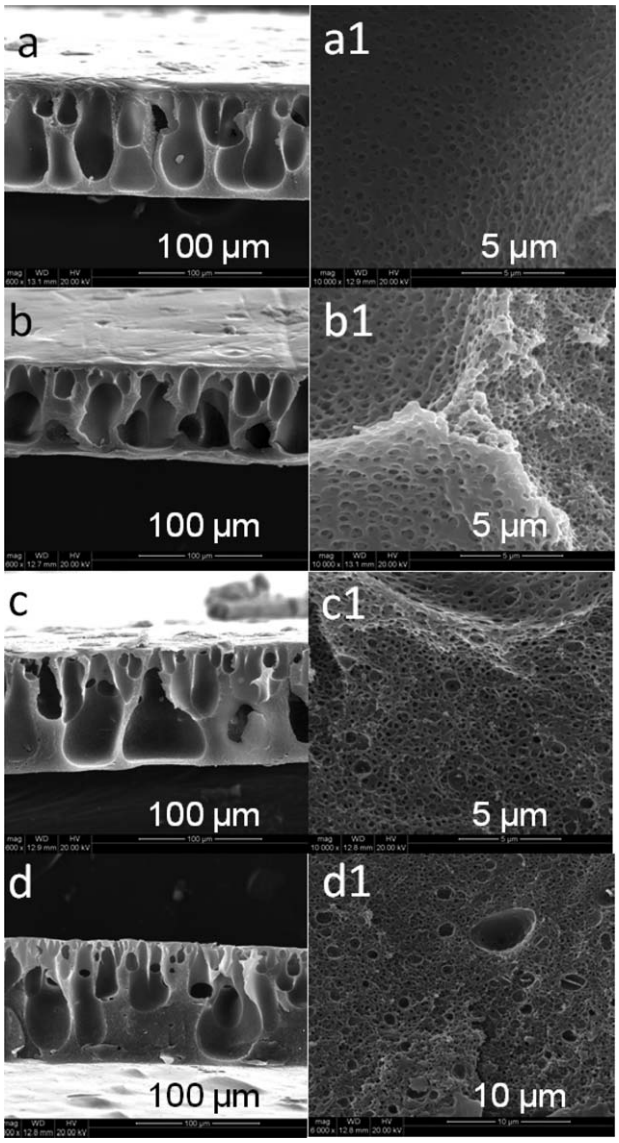

Figure 3. Cross-sectional SEM images of the CNC/CA membranes with different CNC loadings: (a,a1) pure CA membrane, (b,b1) 0.2 wt % CNC, (c,c1) 0.5 wt % CNC, and (d,d1) 1.2 wt % CNC.

images of the membranes. The macropores were well distributed on the bottom surface of both membranes. The CNC/CA blend membrane exhibited more and larger pores than the pure CA membrane on the bottom surface; this was beneficial for improving the separation performance.

The porosity and water content (hydrophilicity) of various membranes were investigated (Figure 5). Both the porosity and water content increased at the beginning. The water content reached its peak value of 72% when the CNC content was 0.5 wt %, and it was 10.9% greater than that of the pure CA membrane (61.1%). The porosity increased by 23.6% from the pure CA membrane (42.8%) to the 0.8 wt % CNC loaded membrane (66.4%). Because the CNCs were prepared by acid-catalyzed hydrolysis of MCC, most of the hydroxyl groups were exposed after the acid hydrolysis, and that improved the hydrophilic properties. During the membrane preparation process, the diffusion between water and solvent (DMAc) was accelerated by the CNCs. The acceleration of the phase-separation process is good for the generation of the polymer-poor phase.[14,29] As evidenced in SEM analysis, the incorporation of CNCs (up to 0.8 wt %) resulted in a higher porosity in the blend membranes. Therefore, the addition of CNCs was beneficial to the formation of membranes with a high porosity and the improvement of hydrophilicity.

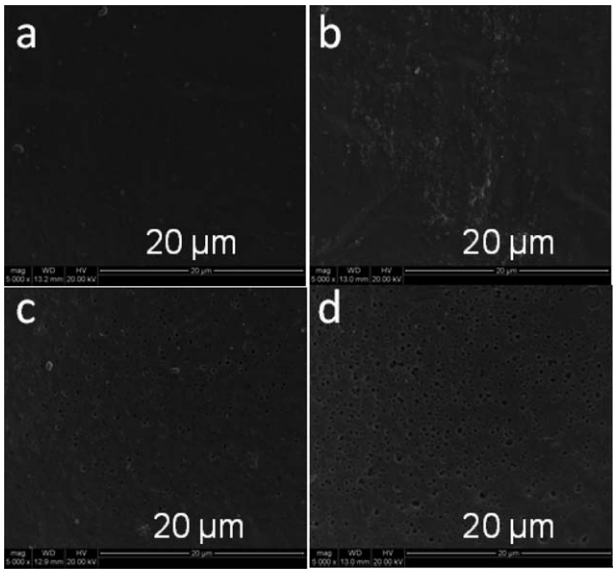

Figure 4. SEM images of the (a,c) pure CA membrane and (b,d) 0.5 wt % CNC blend membrane: (a,b) top surface and (c,d) bottom surface.

Figure 6 shows contact angles of the CA membranes with different CNC loadings. The pure CA membrane had a contact angle of 67.1° [Figure 6(a)], and it had slight hydrophilicity. The contact angle decreased to 53° [Figure 6(b)] after 0.5 wt % CNCs were incorporated; this indicated that the addition of CNCs produced a hydrophilic membrane. Such results were consistent with the water contents of the membranes discussed previously (Figure 5). A further increase in the CNC loading in the CA membrane continuously increased the hydrophilicity of the

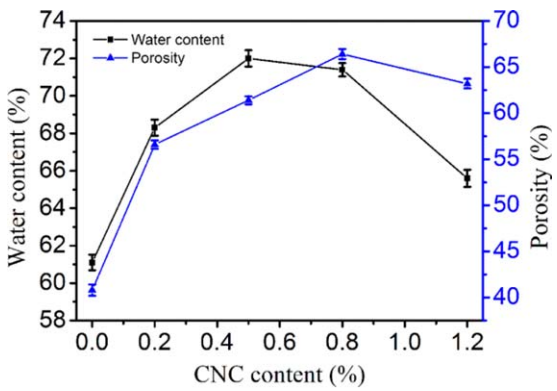

Figure 5. Water content and porosity of the CNC/CA membranes with different CNC loadings. [Color figure can be viewed in the online issue, which is available at wileyonlinelibrary.com.]

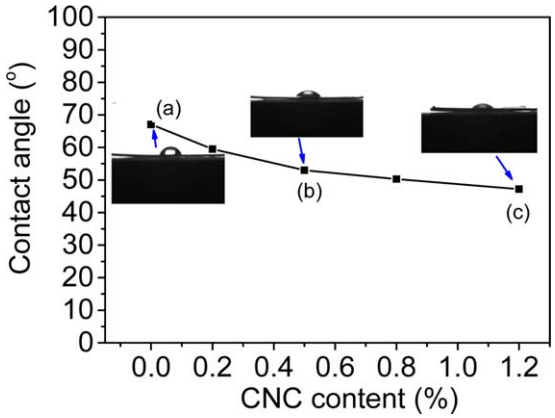

Figure 6. Contact angles of the CNC/CA blend membranes with different CNC loadings. [Color figure can be viewed in the online issue, which is available at wileyonlinelibrary.com.]

membrane, and the contact angle decreased 47.2° with a CNC loading of 1.2 wt % [Figure 6(c)].

Separation and Antifouling Performance

The pure water flux is considered as a key specification factor for ultrafiltration membranes. The pure water flux values of the pure CA and CNC/CA blend membranes were measured after an initial stabilization period of 30 min, and the results are shown in Figure 7. The pure water flux of membrane increased with increasing CNC loading in the casting solution and reached a maximum value of 76 $L\,m^{-2}\,h^{-1}$ when the CNC concentration was 0.5 wt %. The high pure water flux of the CNC/CA blend membranes probably arose from the huge specific surface area and abundant hydroxyl groups on the CNC surface; these were beneficial to the improvement of the hydrophilicity of the CA blend membrane. When the content of CNC was greater than 0.5 wt %, the pure water flux decreased. The aggregated CNCs were poorly dispersed into the CA membrane, forming large unevenly distributed holes in the membrane. These holes did have effects on the membrane permeability, but the impact was slight. This was because the viscosity of the casting solution became higher with more CNC loading, and this led to the agglomeration of CNCs in the casting solution and hindered the process of instantaneous phase separation of the

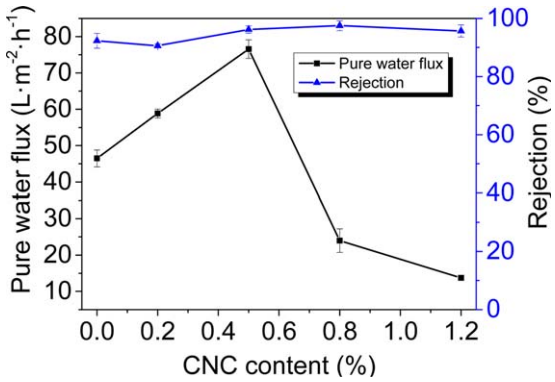

Figure 7. Effect of the concentration of the CNCs on the pure water flux and rejection. [Color figure can be viewed in the online issue, which is available at wileyonlinelibrary.com.]

Table I. Physical Properties of the Blend Membranes

Membrane	Membrane thickness (μm)	Porosity (%)	r_m (nm)
Pure CA	95.0	40.8	68.5
0.2 wt % CNC/CA	127.5	56.6	70.5
0.5 wt % CNC/CA	115	61.4	72.0
0.8 wt % CNC/CA	120	66.4	38.6
1.2 wt % CNC/CA	92.5	63.2	26.7

casting solution, and this reduced the macroporous connectivity of the porous support layer.[29] The rejection ratios of the BSA solution on different membranes were also measured (Figure 7). The results show that all of the BSA rejection ratios remained at a high level, more than 90%. Table I shows the effects of the CNC loadings on the mean pore size of the membranes. The mean pore size of the blend membranes was about 70 nm when the CNC content was less than 0.5 wt %. However, it decreased a lot with increasing CNC content to 1.2 wt %. This indicated that the pure water flux decreased and the BSA rejection ratios were improved when the CNC content was higher than 0.5 wt %.

Membrane pollution can reduce the permeation efficiency and limit the application of ultrafiltration membranes. Thus, the antifouling properties of the membranes were tested, and the results are shown in Figure 8. Membrane cleaning is often used to recover the flux, and an FRR value was introduced to evaluate membrane antifouling properties. The higher the FRR value was, the better the antifouling properties of the membrane were.[7] The FRR value of the pure CA membrane was 60.18%, and the values increased to 68 and 72.24% with the addition of 0.5 and 1.2 wt % CNCs, respectively. Meanwhile, to study deep fouling theory, the fouling resistance characteristics, surface fouling (reversible) and internal membrane fouling (irreversible) rate, of the pure CA and CNC/CA blend membranes were measured. The surface fouling rates of the 0.5 and 1.2 wt % CNC/CA membranes were 38.4 and 42%, respectively; these values were higher than that of the pure CA membrane (35%). We further observed that the extent of the irreversible fouling rate decreased with the addition of CNCs. The original R_{ir} value for the pure CA membrane was 39.82%, and it decreased to 32%

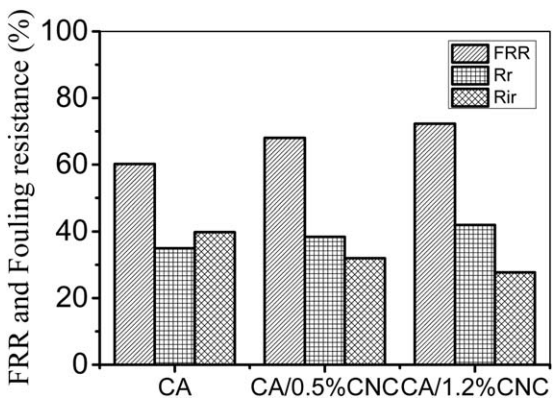

Figure 8. FRR and fouling resistance of the blend membranes.

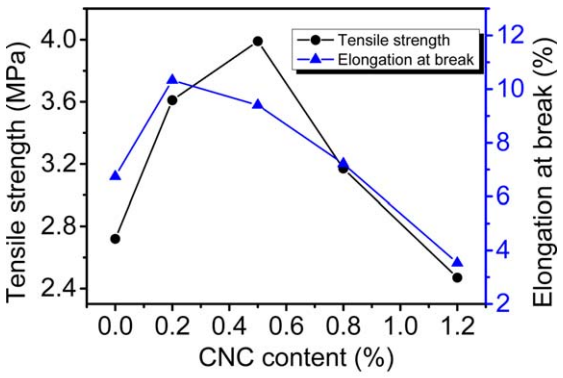

Figure 9. Effect of the concentration of CNCs on the mechanical properties. [Color figure can be viewed in the online issue, which is available at wileyonlinelibrary.com.]

for the 0.5 wt % CNC blend membrane and to 27.76% for the 1.2 wt % CNC blend membrane. This could be explained by the fact that the increase in CNC loadings resulted in the hydrophilicity of the membrane, and this led to a decrease in the protein adsorption. The increase in the FRR value suggested that the CNC/CA membrane fouling was more reversible.

Mechanical Properties

The mechanical properties, including the tensile strength and elongation at break, of the composite membranes are displayed in Figure 9. The tensile strength of the CNC/CA blend membranes reached a peak value of 4 MPa when the CNC content was 0.5 wt %; it increased 47% compared to that of the pure CA membrane (2.72 MPa). The elongation at break also reached a maximum when the CNC content was 0.2 wt %. However, with further increases in the CNC loading, both the tensile strength and elongation at break of the blend membranes decreased a lot and were even worse than those of the pure CA membrane. This suggested that the addition of an appropriate amount of CNCs could improve the mechanical performance of CA membranes. CNC crystals have outstanding mechanical properties, including a high strength and stiffness. They are generally used as reinforcing fillers in polymer composites.[31] In addition, the surface hydroxyl groups of CNCs form a hydrogen-bonding network with the hydroxyl groups of the CA matrix because of their similar structure.[32,33] On the other hand, CNC agglomeration weakened the mechanical properties of the membranes because of the formation of large holes in the blend membranes, which was also evidenced by SEM analysis. According to the previous experimental results, the CNC/CA blend membranes with a comprehensive performance had a CNC loading of 0.5 wt %.

CONCLUSIONS

In this study, CNC-modified CNC/CA ultrafiltration membranes were prepared by a phase-inversion technique with PVP as the additive. The pure CA membrane and the as-prepared blend membranes exhibited a typical asymmetric structure, which was composed of spongelike dense layer and a fingerlike macroporous support layer. We observed that the porosity increased and showed more interconnection with the addition of CNCs compared with the pure CA membranes. The pure water flux of the membranes increased with increasing CNC loading and reached a maximum value of 76 $L\,m^{-2}\,h^{-1}$ when the CNC loading was 0.5 wt %, and the BSA rejection ratio remained at a high level (>90%). Furthermore, the antifouling properties of the CA membrane were improved significantly after the addition of CNCs. In comparison with that of the pure CA membranes, the tensile strength of the composite membranes increased by 47%.

ACKNOWLEDGMENTS

This work was supported by the Natural Science Foundation of Jiangsu Province (contract grant number BK 20141469). The authors gratefully acknowledge the Advanced Analysis and Testing Center of Nanjing Forestry University. One of the authors (J.Y.) acknowledges the support of the Jiangsu Specially Appointed Professor Program.

REFERENCES

1. Zhao, X.; Su, Y.; Li, Y.; Zhang, R.; Zhao, J.; Jiang, Z. *J. Membr. Sci.* **2014**, *450*, 111.
2. Moghadam, M. T.; Lesage, G.; Mohammadi, T.; Mericq, J.; Mendret, J.; Heran, M.; Faur, C.; Brosillon, S.; Hemmati, M.; Naeimpoor, F. *J. Appl. Polym. Sci.* **2015**, *132*, DOI: 10.1002/app.41731.
3. Zhang, F.; Zhang, W.; Yu, Y.; Deng, B.; Li, J.; Jin, J. *J. Membr. Sci.* **2013**, *432*, 25.
4. Reid, K.; Dixon, M.; Pelekani, C.; Jarvis, K.; Willis, M.; Yu, Y. *Desalination* **2014**, *335*, 108.
5. Zhao, Y.; Zhang, P.; Sun, J.; Liu, C.; Yi, Z.; Zhu, L.; Xu, Y. *J. Colloid Interface Sci.* **2015**, *448*, 380.
6. Shi, Q.; Su, Y.; Ning, X.; Chen, W.; Peng, J.; Jiang, Z. *J. Membr. Sci.* **2010**, *347*, 62.
7. Kanagaraj, P.; Neelakandan, S.; Nagendran A. Korean *J. Chem. Eng.* **2014**, *31*, 1057.
8. Krishnamoorthy, L.; Arif, P. M.; Ahmedkhan, R. *J. Mater. Sci.* **2011**, *46*, 2914.
9. Mahendran, R.; Malaisamy, R.; Mohan, D. R. *Polym. Adv. Technol.* **2004**, *15*, 149.
10. Shenvi, S.; Ismail, A. F.; Isloor, A. M. *Ind. Eng. Chem. Res.* **2014**, *53*, 13820.
11. Sivakumar, M.; Mohan, D. R.; Rangarajan, R. *J. Membr. Sci.* **2006**, *268*, 208.
12. Ye, S. *Biomaterials* **2003**, *24*, 4143.
13. Chen, W.; Su, Y.; Zheng, L.; Wang, L.; Jiang, Z. *J. Membr. Sci.* **2009**, *337*, 98.
14. Arthanareeswaran, G.; Sriyamunadevi, T.; Raajenthiren, M. *Sep. Purif. Technol.* **2008**, *64*, 38.
15. Han, B.; Zhang, D.; Shao, Z.; Kong, L.; Lv, S. *Desalination* **2013**, *311*, 80.
16. Habibi, Y. *Chem. Soc. Rev.* **2014**, *43*, 1519.
17. Ganster, J.; Fink, H. *Cellulose* **2006**, *13*, 271.
18. Goetz, L.; Mathew, A.; Oksman, K.; Gatenholm, P.; Ragauskas, A. *J. Carbohydr. Polym.* **2009**, *75*, 85.

19. Zhang, Z.; Wu, Q.; Song, K.; Ren, S.; Lei, T.; Zhang, Q. ACS Sustain. *Chem. Eng.* **2015**, *3*, 574.
20. Saljoughi, E.; Mohammadi, T. *Desalination* **2009**, *249*, 850.
21. Mahdavi, H.; Shahalizade, T. *J. Membr. Sci.* **2015**, *473*, 256.
22. Rahimpour, A.; Madaeni, S. S.; Mansourpanah, Y. *Desalination* **2010**, *258*, 79.
23. Chen, F.; Sun, Z. *Carbohydr. Polym.* **2013**, *95*, 85.
24. Peng, J.; Su, Y.; Chen, W.; Shi, Q.; Jiang, Z. *Ind. Eng. Chem. Res.* **2010**, *49*, 4858.
25. Zhang, L.; Chen, G.; Tang, H.; Cheng, Q.; Wang, S. *J. Appl. Polym. Sci.* **2009**, *112*, 550.
26. Kong, L.; Zhang, D.; Shao, Z.; Han, B.; Lv, Y.; Gao, K.; Peng, X. *Desalination* **2014**, *332*, 117.
27. Zinadini, S.; Zinatizadeh, A. A.; Rahimi, M.; Vatanpour, V.; Zangeneh, H. *J. Membr. Sci.* **2014**, *453*, 292.
28. Alemdar, A.; Sain, M. *Bioresour. Technol.* **2008**, *99*, 1664.
29. Bai, H.; Wang, X.; Zhou, Y.; Zhang, L. *Prog. Nat. Sci. Mater. Int.* **2012**, *22*, 250.
30. Tang, H.; Zhang, L.; Li, S.; Zhao, G.; Qin, Z.; Sun, S. *Spectrosc. Spect. Anal.* **2010**, *30*, 630.
31. Habibi, Y.; Lucia, L. A.; Rojas, O. *J. Chem. Rev.* **2010**, *110*, 3479.
32. Spoljaric, S.; Salminen, A.; Luong, N. D.; Seppälä, J. *Cellulose* **2013**, *20*, 2991.
33. Roohani, M.; Habibi, Y.; Belgacem, N. M.; Ebrahim, G.; Karimi, A. N.; Dufresne, A. *Eur. Polym. J.* **2008**, *44*, 2489.